

Properties of the Kinetochores In Vitro.

II. Microtubule Capture and ATP-dependent Translocation

T. J. MITCHISON and M. W. KIRSCHNER

Department of Biochemistry, University of California, San Francisco, California 94143

ABSTRACT We have studied the interaction of preformed microtubules (MTs) with the kinetochores of isolated chromosomes. This reaction, which we call MT capture, results in MTs becoming tightly bound to the kinetochore, with their ends capped against depolymerization. These observations, combined with MT dynamic instability, suggest a model for spindle morphogenesis. In addition, ATP appears to mobilize dynamic processes at captured MT ends. We used biotin-labeled MT seeds to follow assembly dynamics at the kinetochore. In the presence of ATP and unlabeled tubulin, labeled MT segments translocate away from the kinetochore by polymerization of subunits at the attached end. We have termed this reaction proximal assembly. Further studies demonstrated that translocation could be uncoupled from MT assembly. We suggest that the kinetochore contains an ATPase activity that walks along the MT lattice toward the plus end. This activity may be responsible for the movement of chromosomes away from the pole in prometaphase.

In the preceding paper (24), we described two functional properties of the kinetochore in vitro: microtubule (MT)¹ nucleation and tubulin binding. In neither case was the physiological significance of the in vitro property clear. Indeed, we questioned the relevance of nucleation of MTs at the kinetochore to processes in normal spindle morphogenesis. Although evidence from electron microscopy is equivocal on this point, it supports the idea that the kinetochore can interact with preformed MTs to form the kinetochore fiber (25, 28, 30–32, 39, 41), at least as strongly as implicating a role for kinetochore-based nucleation (4, 8, 35, 44). To approach the question of MT capture by kinetochores, we have studied the interaction of isolated chromosomes with preformed MT in vitro under conditions in which nucleation does not occur. We discuss the question of spindle morphogenesis in light of these results and the newly discovered dynamic properties of MTs (21–23, 37, 38).

Classic studies of Inoue and Sato (16) have shown that the metaphase spindle is a highly dynamic structure in vivo, and that its length can be altered by manipulating the dynamic equilibrium between tubulin dimer and MTs. The dynamic nature of the kinetochore fiber is especially evident during prometaphase, when the bulk of chromosome motility occurs

(3, 26, 35), and during anaphase, when the chromosomes move toward the poles. In the complex spindles of higher eucaryotes, the location of the end of the kinetochore MTs distal to the chromosome is not clear, though many run to the poles (31, 45). However, in the simpler spindles of lower eucaryotes, the kinetochore MTs run continuously from pole to kinetochore, and in these species they too shorten during anaphase (29, 34). Thus, during dynamic changes at all stages of mitosis, it is apparent that the kinetochore MTs can change their length while remaining attached at the kinetochore and probably also the pole. The site(s) at which kinetochore MTs add and lose subunits have yet to be determined, and this knowledge will be crucial in understanding spindle mechanics. Subunit addition and loss are likely to be separate, irreversible reactions (36), and since they do not occur at free MT ends, mechanistically complex.

In this study, we develop assays to examine the dynamics of the MT end attached to the kinetochore in vitro. We observe that the kinetochore may cap the MT against disassembly. In addition, the kinetochore may be able to interact along the length of MTs and catalyze an ATP-dependent translocation process.

MATERIALS AND METHODS

Organelle Preparation: For all the experiments in this paper, we used chromosomes from Chinese hamster ovary cells that were arrested with

¹ *Abbreviations used in this paper:* DTT, dithiothreitol; EGS, ethyleneglycol-bis-succinimidylsuccinate; MT, microtubule; PB, 80 mM PIPES, 1 mM MgCl₂, 1 mM EGTA pH 6.8 with KOH.

10 $\mu\text{g/ml}$ vinblastine sulfate for 11–13 h, isolated as described (24), and stored at -80°C for up to 2 mo. Phosphocellulose-purified tubulin, N115 centrosomes (21), and *Tetrahymena* axonemes (22) were prepared and stored as described.

Preparation of Biotinylated GTP γ S Tubulin: Tubulin was assembled in glycerol assembly buffer and reacted with *N*-hydroxysuccinimidyl biotin (Polysciences, Inc., Warrington, PA) as described (22) with the addition of 2 $\mu\text{Ci/ml}$ of [^3H]GTP (Amersham Corp., Arlington Heights, IL), which was allowed to equilibrate with the tubulin E site before assembly. The biotinylated MTs were sedimented through 50% wt/vol sucrose in 80 mM PIPES, 1 mM MgCl_2 , 1 mM EGTA pH 6.8 with KOH (PB) at 35°C without nucleotide as described, and resuspended at $\sim 5\text{ mg/ml}$ in PB + 2 mM GTP γ S (Boehringer Mannheim Diagnostics, Inc., Houston, TX) + 2 mM dithiothreitol (DTT) at 0°C . After 15 min at 0°C for depolymerization and a cold spin (150,000 g, 20 min, 4°C), MTs were assembled in 33% vol/vol glycerol, 80 mM PIPES, 1 mM MgCl_2 , 1 mM EGTA, 2 mM GTP γ S, 2 mM DTT, pH 6.8 with KOH, at 37°C for 90 min. They were again sedimented through sucrose as above and resuspended at $\sim 10\text{ mg/ml}$ in PB + 1 mM GTP γ S + 1 mM DTT at 0°C by gentle sonication. The solution was sedimented for 10 min in the airfuge (Beckman Instruments, Palo Alto, CA) at 90,000 g, 8°C , and the supernatant was frozen in aliquots with liquid nitrogen and stored at -80°C . GTP γ S tubulin made by this protocol (whether biotinylated or not) contained $<2\ \mu\text{M}$ residual GDP from the initial 1 mM GTP (by scintillation counting), indicating efficient displacement of E site nucleotide. A portion of the tubulin before freezing was brought to a final buffer of 33% vol/vol glycerol, 80 mM PIPES, 1 mM MgCl_2 , 1 mM EGTA, 1 mM GTP γ S, 1 mM DTT pH 6.8 with KOH at a final concentration of 65 μM tubulin. This mixture was frozen in aliquots and stored as above. The labeled MTs used in the proximal assembly experiments (which averaged 4 μm in length) were made by thawing an aliquot of this mixture and incubating it at 37°C for 1 h. We have examined biotinylated GTP γ S MTs polymerized in the buffer described by thin section electron microscopy, and confirmed that the majority have a normal morphology (data not shown).

Fixation and Staining of MT–Chromosome Complexes: We found that glutaraldehyde fixation caused nonspecific cross-linking of free MTs to all portions of the chromosome. We avoided this problem by using a bifunctional protein cross-linking agent, ethyleneglycol-bis-succinimidylsuccinate (EGS) (Pierce Chemical Co., Rockford, IL) (1) to fix MT–chromosome complexes. EGS had been used previously to fix MTs (19). Control experiments showed that a population of growing MTs fixed with 1% glutaraldehyde or by the EGS protocol had identical length distributions. EGS fixation has two main advantages over glutaraldehyde: It does not induce autofluorescence, and more importantly in this experiment, it does not induce adventitious aggregation of fixed objects in solution. The main disadvantages of EGS are that it is sparingly soluble and unstable in aqueous solutions. EGS was made up as a 0.1 M stock in dry dimethyl sulfoxide, and the final fixation mixtures contained 10 mM EGS and 10% dimethyl sulfoxide. The EGS stock was either added directly to the mixture to be fixed, or diluted less than 1 min before a small aliquot of reaction mixture was added. The mixture was gently mixed, and fixation proceeded for 5–15 min at 37°C . Fixed MT–chromosome complexes were layered over 40% vol/vol glycerol in PB at 25°C , and sedimented at 16,000 g for 10 min at 25°C onto polylysine-coated coverslips in corex (Corning Glass Works, Corning, NY) tubes modified as described (10). After washing the interface and aspirating the cushion, the coverslips were removed and postfixed in methanol at -20°C for 5 min. MTs were visualized by anti-tubulin immunofluorescence as described (21), with the addition of Hoechst 33258 at 10 $\mu\text{g/ml}$ to the penultimate wash to visualize chromatin. For proximal assembly experiments, biotinylated and unlabeled MTs were visualized using a Texas red–streptavidin protocol (24) or by sequential incubation in rabbit anti-biotin (Enzo Biochem., Inc., New York, NY) (1/100, 20 min), rabbit anti-biotin + mouse anti-tubulin (20 min) and rhodamine isothiocyanate goat anti-rabbit + fluorescein isothiocyanate goat anti-mouse (Cappel Laboratories, Cochranville, PA) using standard immunofluorescence buffers (21). We found that the anti-biotin protocol gave a stronger fluorescent signal from biotinylated MT segments, probably due to the amplification resulting from the use of secondary antibody.

Quantitation of MT–Chromosome Complexes: The number of captured MTs per chromosome was determined directly in the fluorescent microscope, by counting free MT ends emanating from the primary constriction region of the chromosome. Chromosomes were selected for analysis on the basis of Hoechst staining without looking at the rhodamine channel to avoid bias. For proximal assembly experiments, chromosomes were selected with the fluorescein filter and then photographed using Tri-X (Eastman-Kodak Co., Rochester, NY) developed with Diafine. Since biotinylated segments were not visible with this filter, this procedure assured objectivity. Fluorescein and rhodamine images were superimposed by projecting the negatives and tracing, though in some experiments, overexposure of the rhodamine signal allowed all the information to be derived from a single set of negatives, using a weak signal

from the biotinylated MT segments in the rhodamine channel. At least 100 MT segments were measured per time point.

Free MT Capture: MT seeds were made by polymerizing and shearing tubulin in glycerol assembly buffer as described (21). PB containing 1 mM GTP and tubulin was prewarmed for 2 min. Chromosomes were added to 1/10 of the final volume and then MT seeds, to 1/20 of the final volume. The final tubulin concentration was 10 μM . The mixture was incubated at 37°C with occasional gentle agitation. Aliquots were fixed by a 10-fold dilution into EGS solution, sedimented, and analyzed as described above. The free MTs were visualized by extensively diluting the fixed reaction mixture, sedimenting them onto polylysine-coated coverslips in the airfuge, and performing anti-tubulin immunofluorescence as described (22).

Capture of Centrosomal MTs: Isolated N115 centrosomes were thawed and diluted fivefold to give a mixture at $\sim 10^7/\text{ml}$ and tubulin at 25 μM in PB + 1 mM GTP. After 12 min at 37°C , chromosomes were added to 1/5 of the final volume ($2 \times 10^7/\text{ml}$) together with prewarmed PB and GTP to make the final tubulin concentration 12 μM . The mixture was incubated at 37°C for 10 min with gentle agitation. An aliquot was removed and fixed with EGS as above, and the remainder was diluted into prewarmed PB + 1 mM GTP + 0.1 mM spermidine HCl, 50 μM spermine HCl (PB + GTP + 0.2 \times PA) to give a final tubulin concentration of 0.25 μM . The mixture was incubated at 37°C with minimal agitation. Aliquots were fixed by the addition of EGS stock, sedimented, and visualized as described above. All pipetting and mixing was done as gently as possible to avoid shearing. A similar protocol was used for experiments with axonemes as nucleating elements, using them at an initial concentration of $\sim 10^8/\text{ml}$. For EM observation, the complexes were fixed with 1% glutaraldehyde and sedimented onto polylysine-treated formvar- and carbon-coated grids attached to coverslips, through a glycerol cushion as above. Rotary shadowing was as described (21).

Proximal Assembly Reaction: The final capture reaction contained biotinylated GTP γ S tubulin at 15 μM (without glycerol), chromosomes diluted fivefold, and biotinylated GTP γ S MTs (made as above) diluted 80-fold in PB + 0.25 \times PA + 2 mM DTT + 1 mM MgCl_2 + 1 mM GTP γ S. The reaction mixture was prepared by prewarming the buffer + tubulin for 2 min and adding the labeled MTs, then the chromosomes which were prewarmed for 1 min. In some experiments, more or less labeled MTs were added. The mixture was incubated at 37°C for 10 min with occasional agitation to allow association of MTs with the kinetochores. To elongate the labeled MTs, the mixture was diluted 20-fold (or more) into a prewarmed (2 min) solution of unlabeled tubulin in a final buffer of PB + 0.1 \times PA + 1 mM DTT + 1 mM MgCl_2 + 1 mM GTP. For proximal assembly reactions, 1 mM ATP (or control nucleotide) + 1 mM extra MgCl_2 was also present. For the hexokinase experiment (Fig. 8), the buffer also contained 50 mM glucose, and at the indicated point yeast hexokinase (Sigma Chemical Co., St. Louis, MO) was added to 16 U/ml final volume. Aliquots of the reaction mixture were fixed by a 10-fold dilution into EGS solutions, sedimented, and analyzed as described above. Free MTs were sedimented and analyzed as described above.

Dissociation of Translocation from Assembly: In experiments where translocation was dissociated from assembly and observed on a coverslip (Fig. 10), labeled seeds were initially captured as described above. They were then elongated as above using 10 μM tubulin and no ATP. The elongation was terminated by adding 12 vol of PB containing 33% vol/vol glycerol + 0.1 \times PA + 1 mM DTT at 37°C , and the chromosomes were sedimented onto uncoated coverslips through PB containing 40% vol/vol glycerol + 0.1 \times PA + 1 mM DTT at 30°C as above. After washing the interface and aspirating the cushion, the coverslips were washed several times in PB + 2 mM taxol + 0.1 \times PA + 1 mM DTT. They were then incubated at 37°C in the same buffer containing 1 mM MgCl_2 + 1 mM ATP, or UTP as a control nucleotide. Coverslips were fixed with EGS followed by methanol and analyzed as above.

RESULTS

Capture of MTs by Kinetochores

The kinetochores of chromosomes isolated from vinblastine-arrested cells do not nucleate MT assembly at tubulin concentrations below 15 μM (24). However, MTs that have already been initiated elsewhere can elongate efficiently below this concentration, although they do exhibit dynamic instability (22). In the experiment shown in Fig. 1, MT seeds were mixed with chromosomes and tubulin at 10 μM , a concentration that promotes extensive elongation of the seeds but does not support kinetochore nucleation. When the mixture was

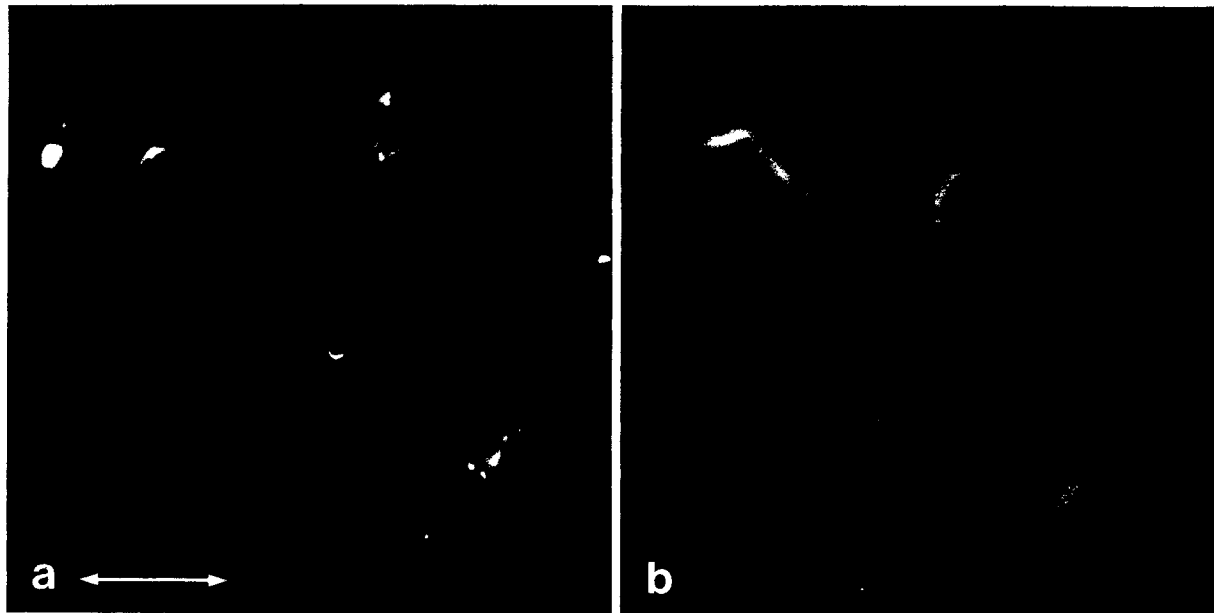


FIGURE 1 Capture of preformed MTs by kinetochores. Chromosomes were incubated in the presence of $10 \mu\text{M}$ tubulin and MT seeds, at the concentration shown by open squares in Fig. 2a. The mixture was fixed after 10 min at 37°C with EGS (see Materials and Methods) and sedimented onto coverslips. Bar, $12 \mu\text{m}$. (a) Anti-tubulin immunofluorescence. Note stained kinetochores with attached MTs. (b) Hoechst 33258 double exposure of the same field. The MTs in a interact only with the primary constriction region of the chromosomes and not the arms. A field containing particularly long chromosomes was selected to emphasize this point.

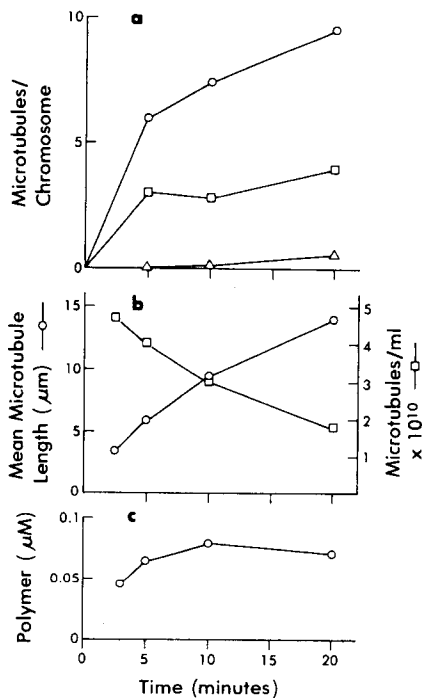


FIGURE 2 Kinetics of MT capture. Chromosomes were incubated in $10 \mu\text{M}$ tubulin at 37°C , and MT seeds were added. At various time points, aliquots were fixed with EGS. (a) The mean number of MTs captured per chromosome. 100 were averaged for each point. ○, mixture seeded with a 1:20 dilution of sheared MT seeds; □, mixture seeded with a 1:60 dilution of sheared MT seeds; △, glycerol assembly buffer without MT seeds added at 1:20 dilution. (b) Data for free MTs in the time points denoted by open circles in a. These data were obtained by sedimenting the free MTs onto coverslips in the airfuge and visualizing them by immunofluorescence. ○, mean MT length. 500 averaged for each time point. □, MT number concentration. 18 photographic fields averaged for

visualized by anti-tubulin immunofluorescence, MTs were found to bind specifically to the kinetochore region of the chromosome. Very few associated with the chromosome arms, as shown in Fig. 1. Many of the MTs appear to interact with the kinetochore by their ends, though this is difficult to determine unambiguously in the light microscope.

The kinetics of MT binding to kinetochores, or capture, are shown in Fig. 2a. Three different initial concentrations of MT seeds were used, and in the sample to which no seeds were added (*open triangles*), very few MTs were seen on kinetochores, confirming the absence of MT nucleation at this tubulin concentration. The kinetics of binding are complicated by the MT dynamics: Most of the free MTs are growing, so their average length increases, but the dynamic instability phenomenon leads to a continuous decrease in number concentration. Fig. 2b shows the changes in mean length and number concentration of free MTs during the incubation. The progressive increase in length and decrease in number will both tend to slow down the rate of association of MTs with the kinetochore, which is reflected by the plateau in the binding curves. In addition, some MTs already associated with the kinetochores may depolymerize. The product of mean length and number concentration, expressed as polymer concentration of free MTs, increases slightly with time, then plateaus (Fig. 2c), indicating that the initial soluble tubulin concentration may be just above the steady state level. The steady state concentration thus appears to be slightly lower here than that previously reported (21), probably because of the small amounts of sucrose (5%) and glycerol

each time point. (c) Total polymer concentration obtained as the product of length and number data in Fig. 2b, assuming 1,700 dimers/ μm . Note that total polymer concentration is always less than 1/10th that of the soluble tubulin ($10 \mu\text{M}$).

(1.5%) present in this experiment. MT-chromosome complexes could also be sedimented through glycerol unfixed under identical conditions (the glycerol cushion acts as an MT-stabilizing buffer), and then fixed on the coverslip with glutaraldehyde or EGS. Similar numbers of MTs were found associated with the kinetochores of chromosomes sedimented fixed and unfixed in parallel. The persistence of the association during sedimentation without cross-linking argues that the MTs are tightly bound. We have also observed that taxol-stabilized MTs can be captured in the virtual absence of soluble tubulin, indicating that MT growth is not required for the binding.

We have used the data of Fig. 2 to estimate a second-order rate constant for the association of MTs with kinetochores. Considering the *open circles* at 5 min, MTs are associating at ~ 0.5 per kinetochore per minute. At an MT concentration of $4 \times 10^{10}/\text{ml}$, this corresponds to a rate constant of $1.3 \times 10^8 \text{ M}^{-1}\text{s}^{-1}$ for MTs $6\text{-}\mu\text{m}$ long. In collaboration with Hill (15), we have constructed some explicit kinetic models of MT end-

kinetochore interaction, and calculated their predicted diffusion-controlled association rate constants. The observed association rate is consistent with models that consider the entire kinetochore disc to be receptive to MT association, at a rate controlled only by MT diffusion. It is too fast for models which posit small (<10) numbers of discrete association sites or larger number of discrete sites (<50) if they require tight angular dependence in the association reaction.

After observing capture of MTs from solution, we were concerned that this might explain the phenomena referred to in the previous paper as MT nucleation. We examined the formation of spontaneous MTs in a typical nucleation assay (24) by sedimentation as described above. Although free MTs were formed above the steady state concentration, at tubulin concentrations below $35 \mu\text{M}$, they did not attain the number concentration required for significant capture. In addition, deliberately adding seeds to a nucleation reaction did not increase the number of MTs at the kinetochore. Thus, nucleation and capture appear to be distinct reactions.

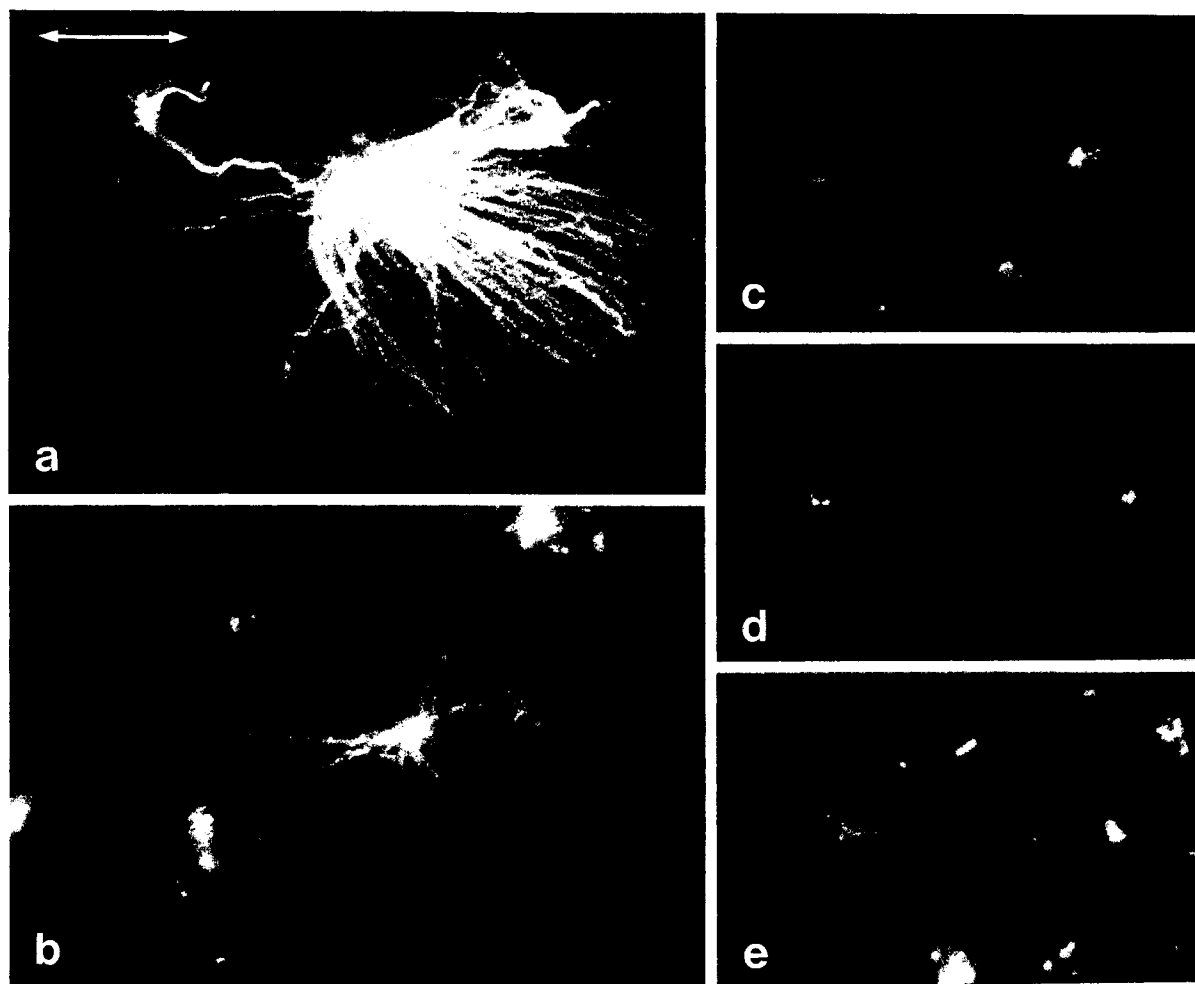


FIGURE 3 Dilution of complexes formed after capture of centrosomal MTs by kinetochores. Centrosomes were incubated with tubulin, and after nucleated MTs had grown to $20\text{--}30 \mu\text{m}$, chromosomes were added. After 12 min, the resulting complexes were diluted to $0.25 \mu\text{M}$ tubulin. (a) Complex formed by incubation of regrown asters with chromosomes, fixed before dilution. The chromosome is the upper left, obscured by surrounding MTs, but visible by Hoechst counter staining (not shown). (b) Complex 40 s after dilution. Uncaptured astral MTs have shrunk to about half their initial length. The connection to the kinetochore is now well visualized, and a single MT can be seen interacting with one of the pair of bright dots. These localized to the primary constriction by Hoechst staining. (c) 90 s after dilution. (d and e) 10 min after dilution. Almost all MTs have depolymerized, and only those stabilized by connections to centrosomes on one end, and kinetochores on the other, are left. The chromosome is to the left in all cases. Bar, $10.5 \mu\text{m}$.

We wished to determine whether the captured MTs were altered in their rates of disassembly at the captured end. To study this, it was necessary to block the distal end so that subunit dynamics would be confined to the end proximal to the kinetochore. This was accomplished by initiating the MT from a nucleating structure, either centrosomes or axonemes, and allowing the free end to be captured by the kinetochore. The stability of the complex was then tested by diluting the sample and evaluating the stability of MTs bound to the kinetochore as compared with the MTs with free ends. In the experiment shown in Fig. 3, MT regrowth was initiated off centrosomes. After the MTs had grown out to 20–30 μm , chromosomes were added, and the mixture was incubated to allow interaction. An aliquot fixed at this stage and sedimented is shown in Fig. 3*a*. The centrosomes had nucleated large, uniform asters of MTs, some of which appear to have contacted a chromosome in the region of the primary constriction. These complexes were then diluted with warm buffer, which caused rapid depolymerization of uncapped MTs (Fig. 3, *b–e*). The captured MTs, however, appear to be much more stable. In the sample fixed 10 min after dilution (Fig. 3, *d* and *e*), the only remaining MTs appeared to connect centrosomes (now visualized by the tubulin staining of the centriole cylinders) to the kinetochore region of chromosomes. Most commonly a single stable MT was observed, (Fig. 3*d*), but sometimes multiple MTs made the connection (Fig. 3*e*). It thus appears that centrosomes cap the MTs they nucleate, and interestingly, kinetochores cap at least some of the MTs they capture. Furthermore, the MT lattice seems to be stable against subunit dissociation from its walls.

The fraction of chromosomes participating in stable complexes with centrosomes was very low (<1%), presumably because both organelles were present at low concentration. However, we routinely observed at least 100 complexes per coverslip. More efficient capture could be achieved using axonemes as the nucleating element, since they could be prepared as a more concentrated suspension. MTs were elongated off the ends of axonemes, incubated with chromosomes to allow capture, and then diluted. 3 min after dilution, between 10 and 30% of the chromosomes were found in stable complexes with axonemes linked by single MTs (see Fig. 4, *a* and *b*). This experiment also allowed us to assess the polarity of capture and capping by sedimenting the complexes remaining after dilution onto electron microscopic grids and using structural cues in the axoneme to assess polarity (2). Examples of two such complexes, one of each polarity visualized by rotary shadowing, are shown in Fig. 4. Since complexes of both polarities were observed, it seems that the capture and cap reaction, like kinetochore nucleation (24), does not manifest a polarity specificity.

Since the complexes formed between centrosomes and kinetochores are analogous to the structure of the mitotic spindle, we were interested in whether any shortening of the connecting MT could be observed. Length measurements showed that although the number of complexes decreased slowly with time after dilution, the mean centrosome–kinetochore distance remained constant. Interestingly, if the initial mixture was diluted into ATP-containing buffers, complexes were never found, and ATP addition to complexes diluted in its absence leads to their rapid disappearance. A similar result was obtained with axoneme–kinetochore complexes. No intermediates were found in this disappearance, so we tenta-

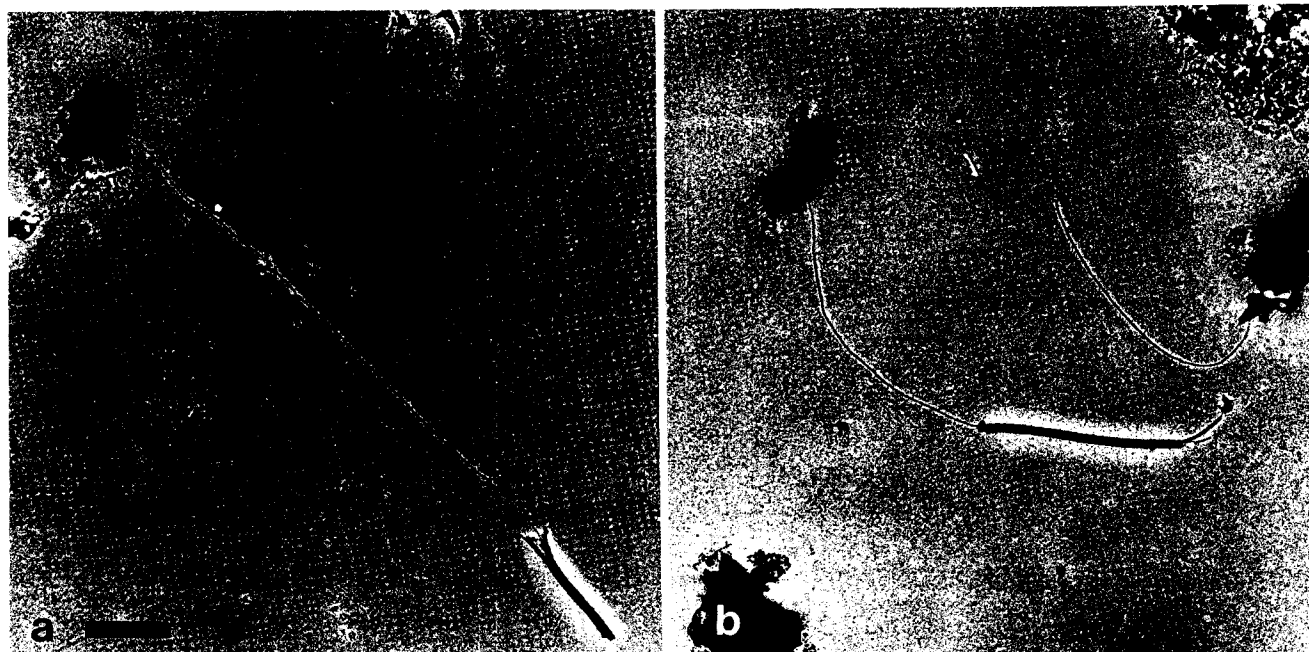


FIGURE 4 Axoneme–kinetochore complexes after dilution. Axoneme–kinetochore complexes were formed as in Fig. 3, except that MT assembly was initiated off axonemes. They were diluted and fixed with glutaraldehyde after 3 min. After sedimentation onto EM grids, complexes were visualized by rotary shadowing. The chromosome is the electron dense structure to the left in both *a* and *b*. Bar, 2.5 μm . (*a*) Axoneme plus end proximal to kinetochore. Note characteristic fraying of the plus end. (*b*) Axoneme minus end proximal to kinetochore. Note central pair structure protruding from the (distal) plus end. 33 such complexes were photographed. Of these 19 appeared to show the kinetochore capturing and capping the MT plus end, and 11 the minus end. The remaining 3 were ambiguous.

tively concluded that ATP addition leads to the MT becoming uncapped and rapidly depolymerized. This effect appeared to be specific to ATP; GTP and AMP-PNP were ineffective.

ATP-dependent Proximal Assembly

Since ATP appeared to cause the loss of a captured MT at low tubulin concentrations, we examined its effect under polymerizing conditions. To detect the possible insertion of subunits proximal to the kinetochore, MT segments labeled with biotin and stabilized by liganding with GTP γ S were employed. The off rate of tubulin subunits from a GTP γ S-liganded MT during depolymerization is slower than that of GDP-liganded subunits from a normal MT by one to two orders of magnitude, probably because the triphosphate is not or is only slowly hydrolyzed during MT polymerization (18). In addition, the on rate is considerably slower (data not shown). Thus, unlike the GDP-liganded MTs in Figs. 1 and

2, their number, concentration, and mean length remain constant, facilitating the capture reaction. MTs formed from such subunits can be distinguished from unlabeled MT segments by immunofluorescence with anti-biotin.

In a typical experiment to detect proximal subunit addition, biotinylated GTP γ S MTs were incubated with chromosomes for 10 min, and an average of two to four were captured per kinetochore. The complexes were then diluted into pre-warmed solutions of unlabeled tubulin, in solutions containing GTP to support normal MT assembly, and with or without 1 mM ATP. The mixtures were then fixed at various time points, sedimented onto coverslips, and processed to visualize both the biotinylated segments and total MT lengths. The results shown in Fig. 5, *a* and *b* clearly indicate that in the presence of ATP and unlabeled tubulin, subunits are inserted between the kinetochore and the biotin-labeled GTP γ S MT segment. This form of novel, apparently insertional, assembly we termed proximal assembly. In addition, the free, distal

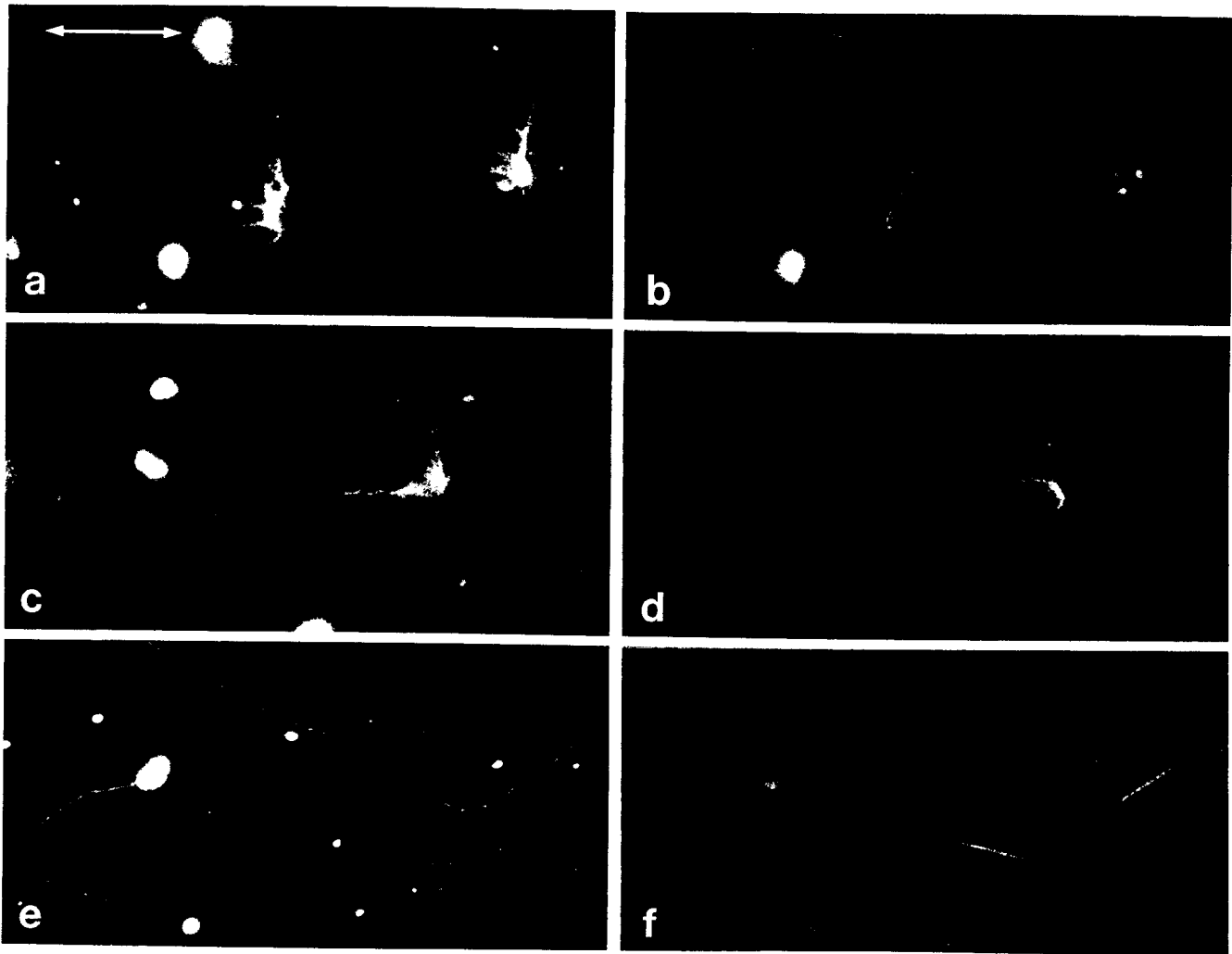


FIGURE 5 Proximal assembly reaction. Biotinylated GTP γ S MTs were captured by kinetochores and then elongated with unlabeled tubulin. (*a*, *c*, and *e*) Total MT visualized with mouse anti-tubulin and FITC goat anti-mouse. (*b*, *d*, and *f*) Only the biotinylated segments visualized with rabbit anti-biotin and RITC goat anti-rabbit. Bar, 12 μ m. (*a* and *b*) Elongation for 5 min in the presence of 1 mM ATP after dilution into 25 μ M tubulin. Note assembly of unlabeled MT segments both proximal and distal to the biotinylated seed. The distal segment is often shorter, reflecting elongation of a minus end. (*c* and *d*) Elongation for 5 min in the presence 1 mM AMP-PNP after dilution into 25 μ M tubulin. Labeled segments remain at the kinetochore and elongate distally. Nucleation of completely unlabeled MT is also seen, as it is in *a* and *b*. (*e* and *f*) Free MT from the reaction shown in *a* and *b*. The uncaptured, biotinylated seeds elongate at both ends and can be used to determine plus and minus end elongation rates. Note also the formation of completely unlabeled MTs by spontaneous polymerization.

ends of the labeled segments elongated as expected, and some nucleation of unlabeled MTs occurred. With GTP alone (or plus UTP or AMP-PNP), the labeled segments remain attached to the kinetochore and elongate by addition of unlabeled tubulin onto the distal ends of captured, labeled segments at the kinetochore (Fig. 5, *c* and *d*).

We considered as an alternative interpretation for the triply segmented MTs attached to the kinetochore, that they resulted from capture of triply segmented free MTs present in the solution that arose from the bipolar elongation of uncaptured seeds (Fig. 5, *e* and *f*). We minimized this possibility by extensive (20 \times) dilution after the initial labeled seed capture, which made free MT capture kinetically highly unfavorable (see Fig. 2). We also performed a control experiment, in which chromosomes were added to the reaction only after the dilution of the labeled seeds into unlabeled tubulin. Using this protocol, less than one chromosome in ten captured a triply segmented MT, whereas the control with chromosomes present initially had an average of 2.1 translocating segments per chromosome. Thus, we favor the interpretation that triply segmented MTs attached to the kinetochore arose by proximal assembly. However, some capture of triply labeled MT is possible with this assay, and the dilution factor into unlabeled tubulin must be maximized to minimize its contribution to the result.

Further analysis of the same experiment yielded both the polarity of translocation and the rate of proximal subunit addition relative to the rate of subunit addition to a free MT end with the same polarity. Uncaptured MTs in the same

solution gave biased bipolar growth (Fig. 5, *e* and *f*). Comparison of the growth rate of the free end of the captured MT with the growth rates of both ends of free MTs gives the polarity of capture. If this segment is then translocated, one obtains the polarity of translocation. Fig. 6 shows length histograms for the unlabeled MT segments that added to the biotinylated seeds at one time point. Elongation of free MTs is shown in Fig. 6*a*, and biased polar growth can be clearly observed, giving a bimodal length distribution with little overlap. The elongation rate of free MTs was unaffected by the presence of ATP or control nucleotide. When 1 mM ATP was present (Fig. 6*b*), translocation occurred, and both proximal and distal unlabeled segments could be measured. The proximal lengths (*hatched bars*) formed a broad distribution, with the longest segments typical of plus end assembly. The distal unlabeled segments (*open bars*) had a sharp distribution, identical to that of the free MT minus ends. We thus conclude that the great majority, or perhaps all, of the proximally assembling MTs had their minus ends distal to the kinetochore. In the absence of ATP (Fig. 6*c*), the captured segments elongated distally at the rates of both plus and minus ends, to give a bimodal length distribution. Thus, there seemed to be little polarity specificity in the initial capture reaction, confirming the observations of axoneme capture mentioned above.

We determined the rates of distal and proximal assembly at three tubulin concentrations onto translocating labeled segments of kinetochore MTs as well as on both ends of free MTs (Fig. 7 and Table I). The mean length of distal assembly onto translocating MTs (*open squares*) was not significantly different from that onto free MT minus ends (*open circles*) at any concentration, confirming the polarity results of Fig. 6. In all cases, very few (always <5%, frequently zero) translocated MTs showed distal addition of plus end length.

The proximal assembly rate increases with tubulin concentration, but is always less than the plus end assembly rate (Fig. 7 and Table I). In no case did we observe a proximally assembled segment longer than the longest free plus end segment at the same time point. The disparity between the

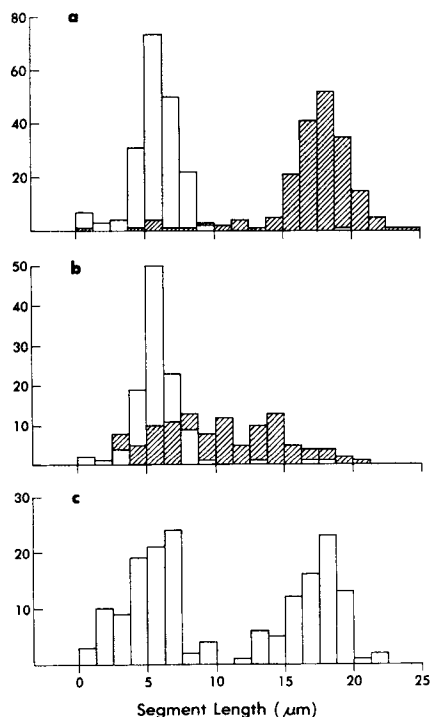


FIGURE 6 Length histograms of unlabeled segments for the experiment shown in Fig. 5. (a) Free MT elongation data; for free MT in sample with ATP. \square , minus ends; \square , plus ends. The longer segment on each MT was assigned as a plus end. 193 MTs total. (b) Chromosome data in 1 mM ATP. \square , distal segments; \square , proximal segments. Note similarity of distal segments to minus end segments in a. 112 MTs total. (c) Chromosome data in 1 mM AMP-PNP. Only distal elongation was seen. 171 MTs total.

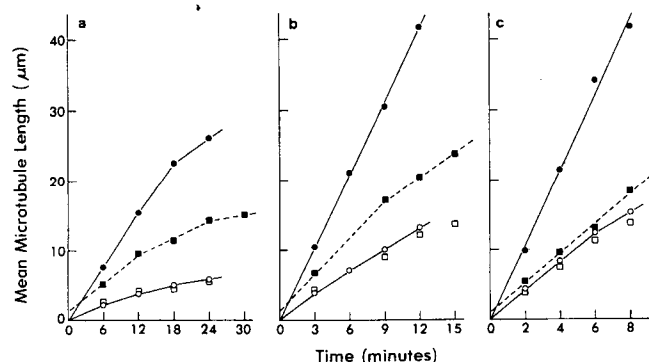


FIGURE 7 MT assembly rates at different tubulin concentrations in the proximal assembly reaction. The reaction conditions were as in Materials and Methods using 1 mM ATP and the indicated tubulin concentration: (a) 10 μ M, (b) 20 μ M, and (c) 30 μ M. 100 each of free and kinetochore MTs were measured at each time point. \bullet , free MTs plus end elongation; \circ , free MTs minus end elongation; \blacksquare , kinetochore proximal assembly segments; \square , kinetochore distal segments on proximally assembling MTs. Continuous lines are drawn through plus and minus end data points from free MTs. Dashed line is through proximal assembly points of kinetochore-associated MTs.

TABLE I. Rate Data Derived from Fig. 7

	Rate data		
	10	20	30
Tubulin concentration (μM)	10	20	30
Free MT plus end assembly rate ($\mu\text{m min}^{-1}$)	1.2	3.4	5.3
Free MT minus end assembly rate ($\mu\text{m min}^{-1}$)	(0.4)	1.2	2.0
Kinetochore MT proximal assembly rate ($\mu\text{m min}^{-1}$)	(0.9)	1.7	2.2
Kinetochore MT distal assembly rate ($\mu\text{m min}^{-1}$)	(0.4)	1.2	1.9
MT plus end rate/proximal assembly rate	1.3	2.0	2.4
MT minus end rate/distal assembly rate	1.0	1.0	1.1

Data were derived by linear regression to the points in Fig. 7, except for the figures in parentheses, which are estimates of initial rates.

free MT plus end rate and the proximal assembly rate increased as tubulin concentration increased (Table I), indicating perhaps that some component of the proximal assembly mechanism other than tubulin polymerization would become rate limiting at sufficiently high assembly rates.

We were interested in determining whether ATP was required continuously for the proximal assembly reaction, or whether ATP activated the process and was only necessary initially. To test this question, proximal assembly was initiated in the presence of ATP and glucose, and then hexokinase was added to an aliquot of the mixture to remove ATP quickly (Fig. 8). We observed that proximal assembly rapidly ceased when hexokinase was added, and the translocated segments remained a constant distance from the kinetochore. Hexokinase has a very low catalytic activity with GTP (7), and consequently MT assembly was unaffected by its addition. This was confirmed using the growth rate of the unlabeled segment distal to the biotinylated seed. We conclude that the continuous presence of ATP is required for the proximal assembly reaction. In addition, we found that proximal assembly is not supported by the nonhydrolyzable ATP analogue, AMP-PNP, and is inhibited by low concentrations of vanadate ($50 \mu\text{M}$, which has no effect on MT assembly). We therefore think it is most likely that translocation involves continuous ATP hydrolysis by an ATPase activity as an integral component.

The proximal assembly phenomenon has not been observed with the mitotic centrosomes that contaminate the chromosome preparation. More surprisingly, we did not observe proximal assembly when the labeled segments were put on the kinetochore by nucleation rather than capture. The reason for this is not known but it is consistent with the idea that capture is the more physiological way of attaching MTs to the kinetochore.

Dissociating Translocation and Assembly

In the previous section, we showed that proximal addition occurs more slowly than does plus end growth but increases with the concentration of tubulin. This suggested that the translocation rate could be limited by the rate of subunit addition, but did not test whether the two processes are obligatorily linked. Under conditions in which the microtubule extended through or past the kinetochore, translocation might become independent of assembly. To test this possibility, assembly onto captured biotinylated GTP γ S segments

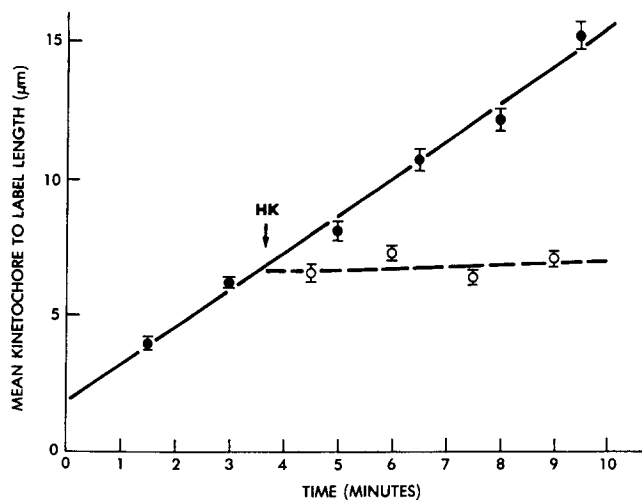


FIGURE 8 Removal of ATP during proximal assembly. Proximal assembly was initiated in buffer containing $22 \mu\text{M}$ tubulin, 1 mM ATP, and 50 mM glucose. At the indicated time point, hexokinase (HK) was added to 16 U/ml . ●, mean length of proximal assembly in the absence of hexokinase; ○, after the addition of hexokinase. More than 100 proximal unlabeled segments were measured per time point, and the error bars show the standard error of the mean.

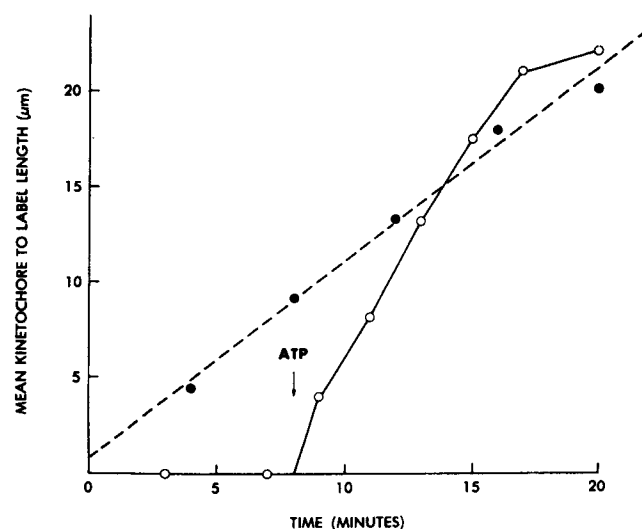


FIGURE 9 Delayed ATP addition. Biotinylated GTP γ S MTs were captured by kinetochores and then elongated with $15 \mu\text{M}$ tubulin in the presence (●) or absence (○) of 1 mM ATP. At the indicated time (8 min), ATP was added to the sample denoted by open circles. Graph shows the mean length of proximal assembled segments, with more than 100 measured per time point. The dotted line was obtained by linear regression through points indicated by closed circles. Linear regression through the first five open circle points after ATP addition gives a translocation rate of $2.3 \mu\text{m/min}$.

was initiated in the absence of ATP, and then ATP was added after 8 min (Fig. 9). A parallel control incubation was performed with ATP present throughout. After delayed ATP addition, the labeled segments appeared to translocate rapidly away from the kinetochore and catch up with the control. This suggested that some kind of proximal assembly had occurred in the absence of ATP, but without translocation. When ATP was added, rapid translocation ensued to move the unlabeled, previously assembled proximal segment away from the kinetochore. This rapid translocation on previously

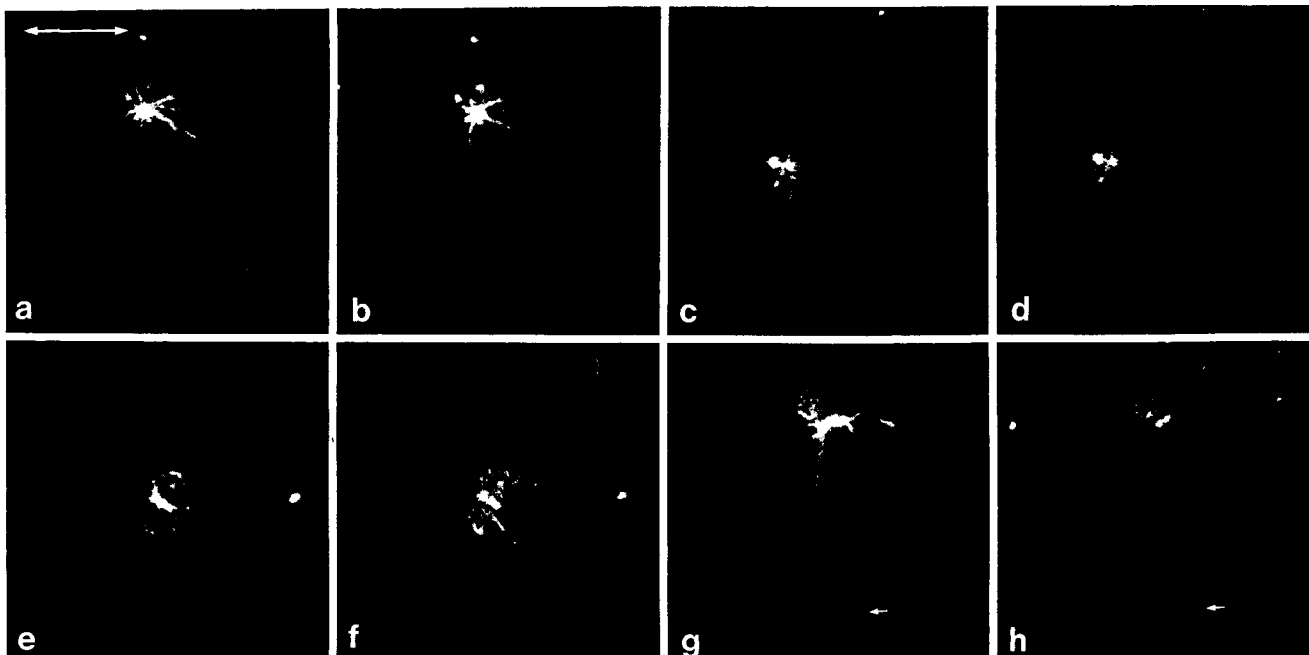


FIGURE 10 Translocation in the absence of MT assembly. Biotinylated GTP γ S seeds were captured by kinetochores and then elongated for 12 min with 10 μ M tubulin and no ATP. They were then sedimented onto coverslips through glycerol-stabilizing buffer, and the coverslips were transferred to taxol-stabilizing buffer without tubulin. The coverslips were then incubated at 37°C for 6 min in this buffer containing 1 mM UTP (a-d) or 1 mM ATP (e-h). Total MT staining is shown in a, c, e, and g, and biotinylated segments in b, d, f, and h. Double exposures are shown of two chromosomes incubated with UTP (a-d) and two with ATP (e-h). Note the translocation of segments in samples incubated with ATP. Many translocated MTs retain distal unlabeled segments: An example is illustrated in g and h, distal to the arrow which indicates the same point in each. Bar, 9 μ m.

assembled polymer seemed to be linear with time, at ~ 2.3 μ m/min. This is faster than the rate of proximal assembly at the highest tubulin concentration in Table I and may represent the maximum possible rate of translocation under these conditions, when assembly is no longer rate limiting.

To determine whether assembly and translocation could be dissociated completely, we isolated a complex of kinetochores and MTs made in the absence of ATP and stabilized with taxol. Then ATP was added in the complete absence of soluble tubulin, and the possible occurrence of translocation observed: Labeled seeds were captured as usual and elongated in the presence of unlabeled tubulin but without ATP, so no translocation occurred. The assembly reaction was stopped by dilution in a MT-stabilizing buffer, and the chromosomes were sedimented unfixed onto untreated coverslips. The coverslips were incubated at 37°C for 6 min in buffers containing taxol and ATP or a control nucleotide (UTP), but no tubulin, and then fixed with EGS and visualized as usual. The results are shown in Fig. 10. In the absence of ATP, labeled segments remained at the kinetochore, with unlabeled segments extending distally (Fig. 10, a-d). With ATP, translocation occurred at high frequency, and many labeled segments were observed at some distance from the kinetochore, connected by an unlabeled segment (Fig. 10, e-h). Many of the segments translocated in the absence of assembly retained distal unlabeled segments (e.g., in Fig. 10, g and h, compare position of arrow), and their lengths usually suggested that the minus end had translocated away from the kinetochore. We have not attempted to use the biased polar assembly assay of polarity in this experiment since MTs may have partially depolymerized to a variable extent in the glycerol-stabilizing buffers. As a statistical check on this experiment, chromo-

TABLE II. Translocation in the Absence of MT Assembly

Conditions	Exp. no.		
	I	II	III
1 mM UTP			
Total chromosomes observed	22	33	25
Total segments counted	90	89	114
Segments translocated	8 (9%)	3 (3%)	3 (3%)
1 mM ATP			
Total chromosomes observed	26	23	20
Total segments counted	74	97	91
Segments translocated	51 (69%)	59 (61%)	54 (59%)
Mean distance of translocation (μ m)	7.9	7.0	8.0

The experiment described in Fig. 10 was repeated three times. An unbiased sample of chromosomes from each coverslip was photographed, and biotinylated segments were scored for translocation relative to the kinetochore.

somes were selected with the fluorescein channel, which had clearly defined MTs attached to the kinetochore. These were photographed, and the frequency with which labeled segments were found translocated away from the kinetochore was determined (Table II). We conclude that taxol-stabilized MTs can slide relative to an immobilized kinetochore in an ATP-dependent reaction.

DISCUSSION

Combining the observations of this and the previous paper (24), we can define five distinct reactions of the kinetochores

of isolated chromosomes *in vitro*: MT nucleation, tubulin binding, MT capture, MT capping, and ATP-dependent translocation. We have shown that nucleation and capture are separate reactions. However, one cannot exclude capture of small tubulin oligomers below the detection level of the light microscope of playing a role in nucleation. In this sense nucleation and capture could be mechanistically related. In particular, both may utilize tubulin binding sites in the fibrous corona.

Morphogenesis of the Kinetochore Fiber

Recently, the observation of the dynamic instability phenomena with centrosomal MTs (21, 22) suggested that the astral array was much more dynamic than previously supposed, and this may have been directly observed by experiments with fluorescent tubulin injection *in vivo* (37, 38). The rapid incorporation of labeled subunits into MTs observed in those studies can be interpreted by the hypothesis that MTs are continuously growing out from the centrosome, becoming unstable through loss of a GTP cap (6), and shrinking back again. Thus, MT ends may continuously probe through the cell. If a trap for MT ends is introduced, it could sequester MTs from the dynamic pool and build up a directed array. In order for such a trap to be effective, it would have to stabilize (at least transiently) the MT ends and prevent their depolymerization. In this study, we have demonstrated these properties for kinetochores. They capture MTs very efficiently, at a rate approaching the diffusion controlled limit. Once captured, the kinetochore confers stability to subunit loss on the MT end (Fig. 3), and thus should act as a trap for dynamic MTs. These ideas are diagrammed in Fig. 11. This model has some useful conceptual features. The first is the idea of morphogenesis by specific stabilization—in this case, the formation of the kinetochore fiber. A directed subset of MTs is formed as a result of random nucleation of a highly dynamic array with spherical symmetry, coupled to specific stabilization of MTs oriented in the required direction. Morphogenesis by capture has the conceptual advantages of not requiring directed growth of MTs or communication from the target to the nucleating element. It could have a role in other cellular morphogenic processes (for further discussion see reference 23). The second advantage of this model is

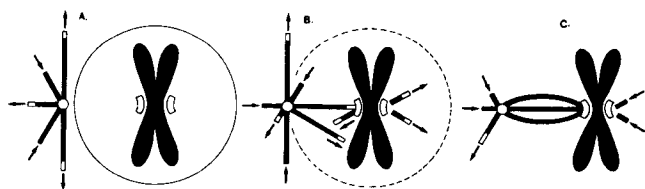


FIGURE 11 Spindle morphogenesis by MT capture. (a) During prophase, highly dynamic astral arrays are formed. MTs are nucleated by centrosomes, grow out with GTP caps (6, 22), and shrink back when these caps are lost. GDP-liganded MTs are denoted by solid line segments, and GTP-liganded subunits are denoted by open line segments. Arrows denote direction of MT assembly. (b) Nuclear envelope breaks down, and kinetochores are exposed to growing MT ends, some of which they capture and stabilize. Nucleation may also occur at kinetochores, but these MTs are likely to disappear by dynamic instability. (c) By metaphase, the kinetochores have captured and stabilized many MTs to form an ordered kinetochore fiber. The polarity of this fiber is specified by the centrosome, with minus ends at the kinetochore.

structural, in that the polarity of the kinetochore fiber is determined only by the nucleating element. Since the centrosome is known to nucleate plus end out MTs with high fidelity both *in vivo* (14) and *in vitro* (5, 24), this aspect of the model economically accounts for the polarity of the kinetochore fiber *in vivo* (9).

An intriguing extension of the model concerns the temporal organization of MTs. Since the kinetochore MTs are removed from the dynamic pool, they will be older on average than the astral MTs. If time-dependent modifications can occur on polymerized MTs, this would allow the chemical differentiation of the older subset (see discussion in reference 26). A time-dependent, polymer-specific modification has been observed in the phosphorylation of β -tubulin in neuronal cells (12), and a time-dependent detyrosination could account for the enrichment of central spindle MTs in α -tubulin lacking the C-terminal tyrosine (13). Such chemical differentiation of kinetochore MTs could help account for their selective depolymerization at anaphase.

Our initial observations of thin section electron microscopy suggest that both end-wise and lateral interaction may occur in the initial capture reaction (data not shown). MT capping could be the result of an initial lateral interaction, followed by depolymerization to a kinetochore-induced block to disassembly. An analogous block may be induced in neural MT by the protein(s) conferring cold stability (43). Since the capping was reversed by ATP, it may be due to the binding of the putative translocating ATPase to the MT lattice.

Dynamics of Kinetochore MTs

In the presence of ATP, we have observed proximal assembly of subunits into MTs at the kinetochore. We interpret the ATP requirement as demonstrating the presence of a translocating ATPase activity at the kinetochore that catalyzes this reaction. The observation of translocation on preformed MTs in the absence of assembly (Fig. 10) suggests that the ATPase does not interact with the MT end, but rather walks along the surface lattice. This would make it mechanistically related to myosin (40) and dynein (17). Such a molecule would be expected to catalyze unidirectional translocation along the lattice, as was observed in proximal assembly experiments (Figs. 6 and 7). Given the polarity that has been determined for the half spindle *in vivo* (9, 14), the observed plus end directed translocation is equivalent to motion away from the pole. These ideas are diagrammed in Fig. 12. The translocating ATPase need not be arranged with any particular geometry in the kinetochore, since the direction of movement would come from the MT lattice. It could be a component of the relatively amorphous corona region, where tight tubulin binding sites have been localized (24). Alternatively, the motile activity in our assays may not in fact be permanently bound to the kinetochore, but rather present as a soluble component, as has been found for reconstituted axonal transport (42).

Attempts to reverse the direction of translocation by depolymerizing the proximal segment were unsuccessful and the labeled segments tended to fall off the kinetochore without translocating. The same dissociation of the kinetochore from the MT end occurred when the stable centrosome-kinetochore complexes (Fig. 3) were exposed to ATP. Taxol-stabilized MTs remain attached after translocation, however (Fig. 10), suggesting that the dissociation may involve the loss of subunits from the MT end.

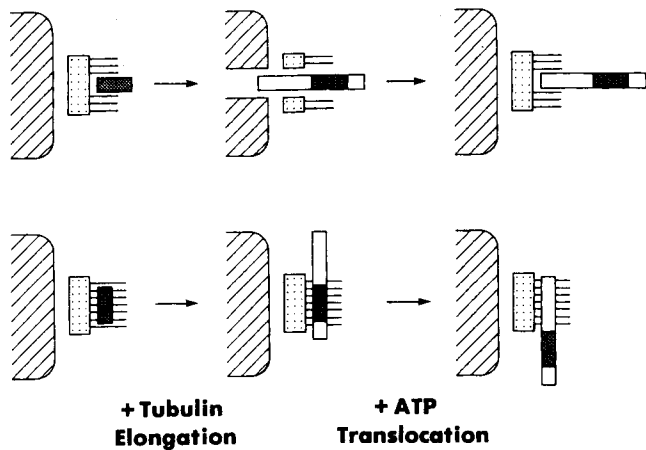


FIGURE 12 Interpretation of dynamics during assembly-translocation experiments. ▨, chromatin; ▩, kinetochore plate; ▨, fibrous corona; □, biotin-labeled MT segment; □, unlabeled MT segment. Labeled MTs may be initially captured by the kinetochore in a variety of orientations, of which two possibilities are shown. In the presence of unlabeled tubulin, they elongate on both ends; the plus end is denoted by the longer unlabeled segment. When ATP is added, the kinetochore translocates toward the MT plus end. This translocation can be simultaneous with (Fig. 5) or subsequent to (Fig. 10) the assembly reaction and is likely to involve an ATPase that walks along the surface of the MT lattice.

Role of Plus End-directed Motility

It is ironic that after spending many hours trying to get chromosomes to move *in vitro*, when they finally did so it was apparently in the wrong direction! However, anaphase movement is only one aspect of mitosis, and in fact, chromosomes exhibit rapid, often oscillatory movements during prometaphase (3, 35). Paired chromosomes frequently cluster around the poles in early prometaphase and must move away from the pole to which they initially attach to reach the metaphase plate (4, 25, 33, 35). This involves extension of the initially short kinetochore fiber, perhaps by proximal assembly at the kinetochore as seen *in vitro*. The major force acting on kinetochores at all stages of mitosis appears to be one of pulling toward the pole to which they are attached (26–28, 35), and achievement of bipolar orientation is a prerequisite for congression to the metaphase plate (4, 25, 35). Thus, the proximal assembly we see may be permissive for kinetochore fiber extension, rather than force generating. However, the oscillations of chromosomes around monopolar spindles (3) and the behavior of diatom spindle during prometaphase (30, 37) suggest that movement of the kinetochore away from the pole may be at least in part an active, force-generating process. Pickett-Heaps, Tippit, and Porter have discussed the relative roles and properties of chromosome-to-pole movements (P) and movements away from the pole (AP) (30). They suggest AP movement may be produced by a dynein-like ATPase, which is consistent with our results. Thus, it seems likely that the translocating ATPase we have defined *in vitro* plays a role in the establishment of the metaphase plate through AP movement. This could occur by proximal assembly of kinetochore MTs, sliding along astral MTs, or both. Since the *in vitro* reaction appeared to be unidirectional, it is less likely to be related to P movement. In addition, the ATPase may be capable of driving a continuous flux of subunits through the kinetochore MTs. MTs

could assemble continuously at the kinetochore during metaphase, and disassemble at the poles, with the lattice being driven polewards by the ATPase. The existence of such a flux has been predicted on both experimental (11) and theoretical (20) grounds. We are currently investigating the sites at which kinetochore MTs add subunits by microinjecting biotin-labeled tubulin into living mitotic cells.

We thank M. Hersh and C. Cunningham-Hernandez for help in preparing the manuscript. We gratefully acknowledge useful discussions and suggestions for improving the manuscript from Z. Cande, T. Hill, K. A. Johnson, B. Lewin, J. R. McIntosh, T. Pollard, E. D. Salmon, and V. Siegel.

This work was supported by grants from the National Institutes of Health and the American Cancer Society.

Received for publication 6 March 1985, and in revised form 1 April 1985.

REFERENCES

- Abdella, P. M., P. K. Smith, and G. P. Royer. 1979. A new cleavable reagent for cross linking proteins. *Biochem. Biophys. Res. Commun.* 87:734–742.
- Allen, C., and G. G. Borisy. 1974. Structural polarity and directional growth of microtubules of *Chlamydomonas* flagella. *J. Mol. Biol.* 90:381–402.
- Bajer, A. S. 1982. Functional autonomy of monopolar spindle and evidence for oscillatory movement in mitosis. *J. Cell Biol.* 93:33–48.
- Bajer, A., and J. Mole-Bajer. 1969. Formation of spindle fibres, kinetochore orientation, and behavior of the nuclear envelope during mitosis in endosperm. *Chromosoma (Berl.)* 27:448–484.
- Bergen, L. G., R. Kuriyama, and G. G. Borisy. 1980. Polarity of microtubules nucleated by centrosomes and chromosomes of Chinese hamster ovary cells *in vitro*. *J. Cell Biol.* 84:151–159.
- Carrier, M. F., T. Hill, and Y.-D. Chen. 1984. Interference of GTP hydrolysis in microtubule assembly: an experimental study. *Proc. Natl. Acad. Sci. USA.* 81:771–775.
- Darrow, R. A., and S. P. Colowick. 1962. Hexokinase from bakers yeast. *Methods Enzymol.* 5:226–235.
- DeBrabander, M., G. Geuens, J. DeMey, and M. Joniau. 1981. Nucleated assembly of mitotic microtubules in living PtK₂ cells after release from nocodazole block. *Cell Motil.* 1:469–483.
- Euteneuer, U., and J. R. McIntosh. 1981. Structural polarity of kinetochore microtubules in PtK₁ cells. *J. Cell Biol.* 89:338–345.
- Evans, L., T. Mitchison, and M. Kirschner. 1985. Influence of the centrosome on the structure of nucleated microtubules. *J. Cell Biol.* 100:1185–1191.
- Forer, A. 1965. Local reduction of spindle fiber birefringence in living *Nephrotoma saturalis* (Loew) spermatocytes induced by ultraviolet microbeam irradiation. *J. Cell Biol.* 25:95–117.
- Gard, D. L., and M. W. Kirschner. 1985. A polymer-dependent increase in phosphorylation of β -tubulin accompanies differentiation of a mouse neuroblastoma cell line. *J. Cell Biol.* 100:764–774.
- Gundersen, G. G., M. H. Kalnoski, and J. C. Bulinski. 1984. Distinct population of microtubules containing tyrosinated and nontyrosinated alpha tubulin are distributed differently *in vivo*. *Cell.* 38:779–789.
- Heidemann, S. R., and J. R. McIntosh. 1979. Visualization of the structural polarity of microtubules. *Nature (Lond.)* 286:517–519.
- Hill, T. 1976. Diffusion frequency factors in some simple examples of transition state theory. *Proc. Natl. Acad. Sci. USA.* 73:679–683.
- Inoue, S., and H. Sato. 1967. Cell motility by labile association of molecules. The nature of mitotic spindle fibres and their role in chromosome movement. *J. Gen. Physiol.* 50:259–292.
- Johnson, K. A., M. E. Porter, and T. Shimizu. 1984. Mechanism of force production for microtubule-dependent movements. *J. Cell Biol.* 99(1, Pt. 2):132s–136s.
- Kirsch, M., and L. R. Yarborough. 1981. Assembly of tubulin with nucleotide analogues. *J. Biol. Chem.* 256:106–111.
- Leslie, R. J., W. M. Saxton, T. J. Mitchison, B. Neighbors, E. D. Salmon, and J. R. McIntosh. 1984. Assembly properties of fluorescein-labeled tubulin *in vitro* before and after fluorescence bleaching. *J. Cell Biol.* 99:2146–2156.
- Margolis, R. L., L. Wilson, and B. Kieffer. 1978. Mitotic mechanisms based on intrinsic microtubule behavior. *Nature (Lond.)* 272:450–452.
- Mitchison, T. J., and M. W. Kirschner. 1984. Microtubule assembly nucleated by isolated centrosomes. *Nature (Lond.)* 312:232–236.
- Mitchison, T. J., and M. W. Kirschner. 1984. Dynamic instability of microtubule growth. *Nature (Lond.)* 312:237–241.
- Mitchison, T. J., and M. W. Kirschner. 1984. Microtubule dynamics and cellular morphogenesis. In *The Cytoskeleton*. D. Murphy, D. F. Cleveland, and G. G. Borisy, editors. Cold Spring Harbor Laboratory, Cold Spring Harbor, NY.
- Mitchison, T. J., and M. W. Kirschner. 1984. Properties of the kinetochore *in vitro*. I. Microtubule nucleation and tubulin binding. *J. Cell Biol.* 101:755–765.
- Mole-Bajer, J. 1975. The role of centrioles in the development of the astral spindle (new). *Cytobios.* 13:117–140.
- Nicklas, R. B. 1971. Mitosis. *Adv. Cell Biol.* 2:225–297.
- Nicklas, R. B., B. R. Brinkley, D. A. Pepper, D. F. Kubai, and G. K. Rickards. 1979. Electron microscopy of spermatocytes previously studied in life: methods and some observations on micromanipulated chromosomes. *J. Cell Sci.* 35:87–104.
- Ostergren, G. 1951. The mechanism of co-orientation in bivalents and multivalents. The theory of orientation by pulling. *Hereditas.* 37:85–156.
- Peterson, J. B., and H. Ris. 1976. Electron microscopic study of the spindle and

- chromosome movement in the yeast *Saccharomyces cerevisiae*. *J. Cell Sci.* 22:219-242.
30. Pickett-Heaps, J. D., D. H. Tippit, and K. R. Porter. 1982. Rethinking mitosis. *Cell*. 29:729-744.
 31. Rieder, C. L. 1981. The structure of the cold stable kinetochore fibre in metaphase PtK₁ cells. *Chromosoma (Berl.)*. 84:145-158.
 32. Rieder, C. L. 1982. The formation, structure and composition of the mammalian kinetochore and kinetochore fiber. *Int. Rev. Cytol.* 79:1-57.
 33. Rieder, C. L., and G. G. Borisy. 1981. Attachment of kinetochores to the prometaphase spindle in PtK₁ cells. *Chromosoma (Berl.)*. 82:693-716.
 34. Roos, U.-P. 1975. Mitosis in the cellular slime mode *Polysphondylium violaceum*. *J. Cell Biol.* 64:480-491.
 35. Roos, U.-P. 1976. Light and electron microscopy of rat kangaroo cells in mitosis. III. Patterns of chromosome behavior during prometaphase. *Chromosoma (Berl.)*. 54:363-385.
 36. Salmon, E. D., and D. A. Begg. 1980. Functional implications of cold-stable microtubules in kinetochore fibers of insect spermatocytes during anaphase. *J. Cell Biol.* 85:853-865.
 37. Salmon, E. D., R. J. Leslie, W. M. Saxton, M. L. Karow, and J. R. McIntosh. 1984. Spindle microtubule dynamics in sea urchin embryos: analysis using a fluorescein-labeled tubulin and measurements of fluorescence redistribution after laser photobleaching. *J. Cell Biol.* 99:2165-2174.
 38. Saxton, W. M., D. L. Stemple, R. J. Leslie, E. D. Salmon, M. Zavortink, and J. R. McIntosh. 1984. Tubulin dynamics in cultured mammalian cells. *J. Cell Biol.* 99:2175-2186.
 39. Schibler, M. J., and J. D. Pickett-Heaps. 1980. Mitosis in *Oedogonium*: spindle microfilaments and the origin of the kinetochore fiber. *Eur. J. Cell Biol.* 22:687-698.
 40. Sheetz, M. P., R. Chasan, and J. A. Spudich. 1984. ATP-dependent movement of myosin in vitro: characterization of a quantitative assay. *J. Cell Biol.* 99:1867-1871.
 41. Sluder, G., and C. L. Rieder. 1985. Experimental separation of pronuclei in fertilized sea urchin eggs: chromosomes do not organize a spindle in the absence of centrosomes. *J. Cell Biol.* 100:897-903.
 42. Vale, R. D., B. J. Schnapp, T. S. Reese, and M. P. Sheetz. 1985. Organelle, bead, and microtubule translocations promoted by soluble factors from the squid giant axon. *Cell*. 40:559-569.
 43. Webb, B. C., and L. Wilson. 1980. Cold stable microtubules from brain. *Biochemistry*. 19:1993-2001.
 44. Witt, P. L., H. Ris, and G. G. Borisy. 1980. Origin of kinetochore microtubules in CHO cells. *Chromosoma (Berl.)*. 81:483-505.
 45. Witt, P. L., H. Ris, and G. G. Borisy. 1981. Structures of kinetochore fibers: microtubule continuity and intermicrotubule bridges. *Chromosoma (Berl.)*. 83:523-540.